September 23, 2018
Preprint typeset using LaTeX style emulateapj v. 11/26/04

DIFFRACTION OF LIGHT AS A LIMITING FACTOR FOR TELESCOPES' ANGULAR RESOLUTION ON THE EXAMPLE OF JAMES WEBB SPACE TELESCOPE

Jowita Borowska
Institute of Theoretical Astrophysics, University of Oslo, P.O. Box 1029 Blindern, N-0315 Oslo, Norway; jowitab@student.matnat.uio.no
Laboratory exercise performed August 30, 2018; Report submitted September 23, 2018

ABSTRACT

Experiments aiming to study diffraction phenomena were conducted using two different laboratory set-ups. First one, allows observation of a single slit Fraunhoffer diffraction pattern and by that, measuring the wavelength of the laser light, $\lambda = 653 \pm 8$ nm. After replacing a slit by a bent paperclip (modelling an "anti"-slit), its thickness is determined, $a_a = 878 \pm 31$ μm.
Thereafter, diffraction by a cricular aperture is being studied. We derive a formula that yields the angular radius of the Airy disk: $\theta_{min} = K\lambda/d$, where K is a constant, estimated to be 1.34 (with approximately 20% uncertainty), λ is a wavelength of light (found for the second laser by using an image of the Airy pattern, equal $\lambda = 673 \pm 70$nm) and d a diameter of an aperture. We arrive at the conclusion, following the Rayleigh's criterion and the above equation, that the angular resolution of any telescope is limited by diffraction and depends on the wavelength, at which it observes, as well as its mirror diameter. Applying that to James Webb Space Telescope, we find its angular resolution to be in the range between $0.028''$ and $0.022'$, then estimate its spatial resolution for various distances.

Subject headings: Airy pattern - diffraction, JWST - angular resolution

1. INTRODUCTION

People have always been fascinated by stars. Throughout the history of mankind we have been trying to understand our place in the Universe and how it began. Science and engineering develop at a tremendous pace, bringing us more and more sophisticated tools to obtain that knowledge. From Galileo's telescope, designed in 1609, to James Webb Space Telescope, planned to be launched in three years' time (NASA 2018), astronomical observations became significantly more accessible and accurate. We have escaped Earth's atmosphere in order to avoid *seeing* - irregular variations of refractive index in the air mass - and be able to observe the wider spectrum of wavelengths, for instance infrared or UV, absorbed by the atmosphere (Thorne & Blandford 2012). Nevertheless, we cannot escape the nature of light and its inevitable consequences. Light exhibits properties of both particles and waves. Diffraction, being a phenomenon associated with the very wave-nature of light, puts a limit on how well any telescope can resolve neighboring objects. Hence the question: how precisely and how far into space can we see? In the following sections we aim to find out what the said limit is. Various diffraction patterns are being studied closer (first by a single slit, then 'anti'-slit and finally, by a circular aperture) to experimentally derive an expression for the angular resolution of a telescope.

2. METHODS

We begin with a very well-controlled situation in which light passes through a single narrow slit (of width 100 μm). The experimental set-up consists of a small laser tube (powered by a 4.5 Volt flat battery), mounted on a simple platform, and the slit mounted on a separate one. By aiming the laser on the slit, we are able to observe a light pattern projected on the wall, called a Fraunhoffer diffraction pattern. Intensity distribution of this pattern is shown on the Figure 1. Clearly, following

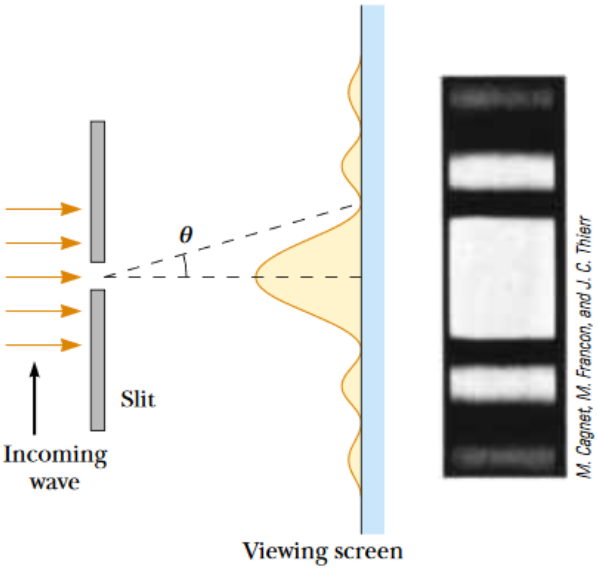

Fig. 1.— The Fraunhoffer diffraction pattern from a single slit, with intensity distribution, from Serway & Jewett (2004).

Huygens'principle, the light intensity is angle-dependent (Serway & Jewett 2004). Flux minima can be observed when

$$\sin(\theta) = \frac{m\lambda}{a}, \tag{1}$$

where a is the slit width, m the order of the minimum and λ the wavelength of the monochromatic laser light. Simple rearrangment of the above formula gives us an expression for the wavelength of the laser, $\lambda = a\ \sin(\theta)/m$. Since the wall, where the pattern occurs, is fairly far from the slit, θ is a very small angle and can be approximated by

(result of truncation of the Taylor series for $\sin(\theta)$ and $\tan(\theta)$)

$$\theta \approx \sin(\theta) \approx \tan(\theta) = \frac{x}{s}, \tag{2}$$

where x is the distance between a reference center of the symmetrical pattern and the last marked minimum, and s is the distance between the slit and the wall. In fact, inserting the actual values obtained form the experiment, it can be verified that the approximation is very accurate in our case ($\tan(\theta) \approx 0.0718$ [rad], $\sin(\theta) \approx 0.0716$ [rad]). The rearranged equation (1) combined with small angle-approximation (2) is then

$$\lambda = \frac{a\sin(\theta)}{m} \approx \frac{a\tan(\theta)}{m} = \frac{ax}{ms}. \tag{3}$$

Uncertainties of the quantities appearing in the formula "propagate" to the uncertainty of the result. When it comes to the λ-measurment, given by formula (3), with multiplication and division, fractional uncertainties add in quadrature, following "Error Propagation" (2007). The error in λ-measurment is then

$$\frac{\delta\lambda}{|\lambda|} = \sqrt{\left(\frac{\delta x}{x}\right)^2 + \left(\frac{\delta s}{s}\right)^2}, \tag{4}$$

as a and m are "certain quantities".

Thereafter, we replace the slit by a bent paperclip and move it further away, simultaneously increasing the distance to the wall. We have already measured the wavelength of the laser, therefore we are able to determine the thickness of the paperclip using the new, "anti"-slit diffraction pattern that is now being projected on the wall (it is similar, but relevantly varies from the one before). Manipulating equation (3) (since the small-angle approximation still holds, as the distance between the paperclip and the wall is even greater), we find that

$$a_a = \frac{m\lambda s}{x}, \tag{5}$$

where a_a is the thickness of the paperclip ("anti"-slit), λ the wavelength and m, s refer to the new diffraction pattern. Again, following "Error Propagation" (2007), the uncertainty of the measurment propagates to

$$\frac{\delta a_a}{|a_a|} = \sqrt{\left(\frac{\delta\lambda}{\lambda}\right)^2 + \left(\frac{\delta x}{x}\right)^2 + \left(\frac{\delta s}{s}\right)^2}. \tag{6}$$

Next set-up we use, includes the laser connected through a fiber to the collimator tube, with dampening filter. Parallel light rays, partially blocked by the filter, are focussed by the doublet lens (which focal length equals 100 mm) and the magnified image of the focal plane is recorded by a mono-chromatic camera. The collimated beam of light (being actually a good representation of a light coming from distant stars) is weakened by dampening filter to protect from strong overexposure and enable camera to record an image of the diffraction pattern. The microscope objective placed together with the camera magnifies its 6μm pixels by a factor of twenty, so that one pixel seen on the image corresponds to 0.3μm in the real scale (1 pixel $\sim 6\mu\text{m}/20 = 0.3\mu\text{m}$).
Precise alignment of the laser tube, lens, microscope objective and the camera has a crucial impact on imaging a diffraction pattern in the focal plane. Once the experimental set-up is correctly positioned, we can record an exposure and observe the resulting Airy pattern - central bright "Airy disk" surrounded by alternately dark and lighter concentric rings which intensity dimninishes with radius (Thorne & Blandford 2012). Again, there is an angle-dependence in the position of flux-minima:

$$\sin(\theta) = \frac{K\lambda}{d}, \tag{7}$$

where λ is the wavelength of laser, d the diameter of the aperture and K is a constant, known for the second minimum, $K = 2.23$. Since we use a different laser, the wavelength of light needs to be measured. By a closer examination of the recorded exposure, we are able to find the precise distance from the center to the second darker ring (2nd flux-minimum), as well as the radius of the Airy disk. Furthermore, we notice that these distances are very small comparing to the focal length, so that equation (2) holds. Hence, the wavelength of light for another laser can be calculated as

$$\lambda = \frac{d\sin(\theta)}{K} \approx \frac{d\tan(\theta)}{K} = \frac{rd}{Kf}, \tag{8}$$

where r is the distance to the second minimum (number of pixels counted on the image multiplied by 0.3μm as explained before) and f is the focal length of the doublet lens (distance between the lens and the image formed in the focal plane). Besides the constant, K, all quantities are burdened with uncertainties, which propagate to ("Error Propagation" 2007)

$$\frac{\delta\lambda}{|\lambda|} = \sqrt{\left(\frac{\delta d}{d}\right)^2 + \left(\frac{\delta r}{r}\right)^2 + \left(\frac{\delta f}{f}\right)^2}. \tag{9}$$

Having measured λ and the radius of the Airy disk, we are now able to assess the value of K for the first minimum. Finding this constant is a highlight of the experimental work done by now, because it determines the angular resoultion of any telescope and we will use it in the further calculations with James Webb Space Telescope as an example. By a simple rearrangement of formula (8),

$$K = \frac{rd}{\lambda f}, \tag{10}$$

where r refers to the position of the first flux-minimum. Error propagation leads to the following uncertainty in the K-assessment:

$$\frac{\delta K}{|K|} = \sqrt{\left(\frac{\delta d}{d}\right)^2 + \left(\frac{\delta r}{r}\right)^2 + \left(\frac{\delta f}{f}\right)^2 + \left(\frac{\delta\lambda}{\lambda}\right)^2}. \tag{11}$$

Subsequent experiments conducted in the laboratory focus on further examination of the Airy pattern and aim to understand the consequences for astronomical observations and telescopes' performance. This includes: reducing the circular aperture, observing the patterns of dust in the optical system and eventually, replacing the lens by a coin and altering the set-up by removing the camera and microscope objective, as well as replacing the part with the dampening filter by the corresponding part of the white light tube.

Finally, experimentally acquired knowledge can be applied to the particular example - James Webb Space Telescope. Formula (7) represents the limiting angle of resolution for a telescope with mirror diameter d, performing observations at the wavelength λ. If the two objects on the sky are closer than this angular resolution, we do not expect a given telescope to fully distinguish them as separate objects (Thorne & Blandford 2012). As the diameter of a primary mirror of JWST is approximately 6 meters and the spectrum of wavelengths in which it will observe is between 600 nm and 28.5 μm (NASA 2018), we can estimate its angular resolution for both extremes of the spectrum. For this purpose, we combine (2) and (7) formulae:

$$\theta_{min} \approx \sin(\theta_{min}) = \frac{K\lambda}{d}. \tag{12}$$

Furthermore, proceeding with small-angle approximation:

$$\theta_{min} \approx \tan(\theta_{min}) = \frac{l}{S} \Rightarrow l = S\theta_{min}, \tag{13}$$

we can find l - the smallest physical size of an object that JWST can resolve from a distance S. Obviously, since the angular resolution is better while observing at smaller wavelengths, we use θ_{min} calculated for orange, 600 nm-light.

When it comes to the uncertainty of two latest estimates, following "Error Propagation" (2007), we find:

$$\frac{\theta_{min}}{|\theta_{min}|} = \sqrt{\left(\frac{\delta K}{K}\right)^2} = \frac{\delta K}{|K|} = \frac{\delta l}{|l|}, \tag{14}$$

as we assume given d, λ and S-values not to be burdened with uncertainties.

3. RESULTS

In the experiments with the smaller laser, the wavelength of light can be calculated using formula (3). We have measured the distance between the center of the symmetric diffraction pattern and the minimum of order $|m| = 11$ to be $x = 9 \pm 0.1$ cm, whereas the distance between the slit and the wall, $s = 125.3 \pm 0.5$ cm. Inserting these values, together with the slit width, $a = 100$ μm, into equation (3) yields $\lambda = 653$ nm. Moreover, using formula (4), we find that the error propagation leads to 1.18% uncertainty in λ-measurment, so that $\lambda = 653 \pm 8$ nm.

Having obtained the wavelength of the laser, we can use the "anti"-slit diffraction pattern to determine the thickness of the paperclip, which has now replaced the slit. Measured quantities are: $|m| = 25$, $x = 3 \pm 0.1$ cm and $s = 161.4 \pm 0.5$ cm. Inserting them into formula (5) and, together with $\delta\lambda/|\lambda| = 0.0118$, into formula (6) results with $a_a = 878 \pm 31$ μm (error propagates to 3.55% uncertainty of a_a-measurment).

Moving on to the second experimental set-up, we are again interested in finding the wavelength of the monochromatic laser light. Complying with the method described above, we record an exposure, which can be seen in the Figure 2. Zoom in on the central part of the image, with clearly visible Airy disk, is also shown in order to enable precise measurment of distances from the center to the frist and second ring, where the flux vanishes. These distances, marked on the Figure 2, are consecutively $6 \cdot 0.3$ μm $= 1.8$ μm and $10 \cdot 0.3$ μm $= 3.0$ μm

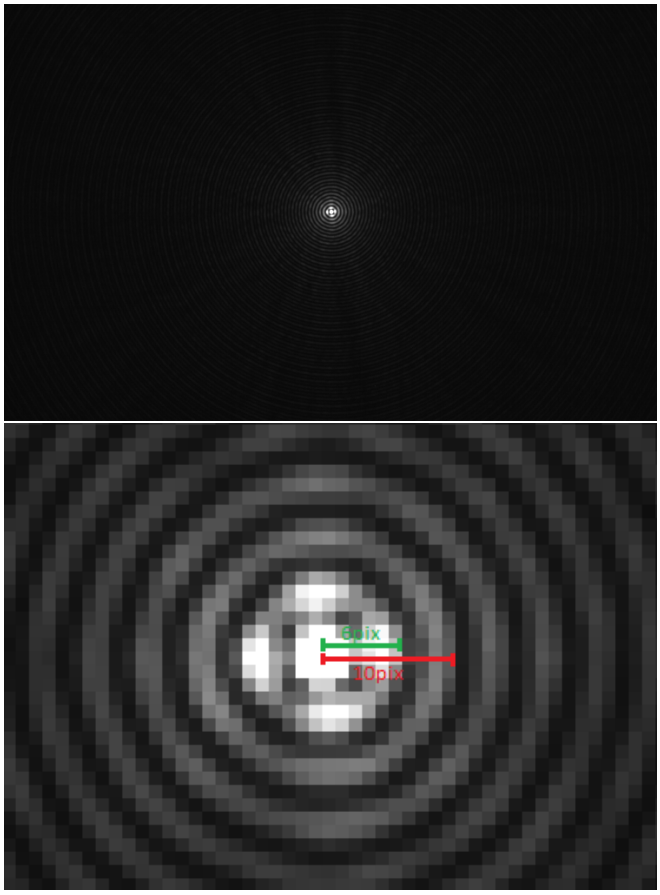

FIG. 2.— The recorded exposure with the Airy pattern. One pixel on the image corresponds to 0.3 μm. Lower picture is a zoom in on the central part of the Airy pattern shown above with marked distances to the 1st and 2nd light flux-minima.

with $\pm$ [one pixel ~ 0.3 μm] uncertainty due to the blurriness.

Using formulae (8) & (9), inserting d = 5.0 $\pm$ 0.1 cm, f = 10.0 $\pm$ 0.2 cm and the quantities corresponding to the second minimum: $K = 2.23$, $r = 3.0 \pm 0.3$ μm, we find that the wavelength is equal $\lambda = 673 \pm 70$nm (resultant from 10.39% uncertainty). To determine the constant K for the first minimum, we insert proper values into the equations (10) & (11):

$$K = \frac{rd}{\lambda f} = \frac{6 \cdot 3.0 \cdot 10^{-7}\ \text{m} \cdot 5.0 \cdot 10^{-2}\ \text{m}}{6.73 \cdot 10^{-7}\ \text{m} \cdot 0.1\ \text{m}} = 1.34,$$

with uncertainty:

$$\frac{\delta K}{|K|} = \sqrt{\left(\frac{\delta d}{d}\right)^2 + \left(\frac{\delta r}{r}\right)^2 + \left(\frac{\delta f}{f}\right)^2 + \left(\frac{\delta \lambda}{\lambda}\right)^2}$$

$$= \sqrt{\left(\frac{0.1}{5}\right)^2 + \left(\frac{1}{6}\right)^2 + \left(\frac{0.2}{10}\right)^2 + (0.1039)^2} = 19.84\%$$

$$\Rightarrow K = 1.34 \pm 0.27$$

(the whole calculation process is shown due to the importance of K-measurment and its further application).

Reduction of the aperture, using the circular aperture reducer, results in the increase of Airy disk size. This consequence could easily be foreseen by the equation (7) - the distance between the center and the minima has to be larger for a smaller diameter of the aperture, d.

Having experimentally derived formula (12), which yields the effective radius of the Airy disk, we find the angular resolution of JWST at extremes of the observed wavelength-spectrum:

- for $\lambda = 600$ nm (orange light):

$$\theta_{600\text{nm}} = \frac{1.34 \cdot 6.0 \cdot 10^{-7} \text{ m}}{6 \text{ m}} = 1.34 \cdot 10^{-7} \text{ [rad]} \approx 0.028'',$$

- for $\lambda = 28.5$ μm (mid-infrared):

$$\theta_{28.5\mu\text{m}} = \frac{1.34 \cdot 2.85 \cdot 10^{-5} \text{ m}}{6 \text{ m}} = 63.65 \cdot 10^{-7} \text{ [rad]} \approx 0.022'.$$

Furthermore, by applying formula (13), we can estimate the smallest size of objects that JWST can resolve during the observations from various distances. Some examples are shown in Table 1. Constant K, calculated before, determines the uncertainty of $\theta_{600\text{nm}}$, $\theta_{28.5\mu\text{m}}$, as well as resolved objects' sizes to be

$$\frac{\theta_{min}}{|\theta_{min}|} = \frac{\delta l}{|l|} = 19.84\%. \qquad \text{eq. (14)}$$

4. DISCUSSION AND CONCLUSION

We have used two different experimental set-ups (alternating the second one in order to observe a different pattern, with Arago spot). The wavalengths of both lasers, measured to be subsequently $\lambda_1 = 653 \pm 8$ nm and $\lambda_2 = 673 \pm 70$ nm, seem to be in agreement with the observations, as in both cases the laser light was evidently in the red-range.

The first diffraction pattern, we observe, consists of the central maximum - intense broad band of light - and a series of less intense and narrower bands (whose intensity decreases with the distance from the center) occuring alternately with dark fringes (minima). The very first formula is based on the destructively interfering light rays, resultant in the mentioned dark fringes with zero intensity (Serway & Jewett 2004).

When the slit is replaced by a bent peperclip, we can observe a similar series of bright bands and intervening dark ones (and also a bright central maximum). Pattern is, however, different from the one before, as the fringes occur more densely - we have counted $|m| = 25$ minima on the span of $x = 3$ cm. Babinet's theorem states that diffraction patterns of complementary diffracting objects outside the central beam are identical (PHYWE 2006). Nevertheless, the thickness of the peperclip is measured to be almost nine times larger than the width of the slit, so the introduced object ("anti"-slit) is not fully complementary with the slit. Resultant diffraction pattern is then, as expected, not the same as the one from a single slit of width a.

The second "shape" of diffraction pattern we observe is the diffraction by a circular aperture, described before and shown on the Figure 2. Based on observations, we can conclude that diffraction pattern resembles the shape of an aperture - we have seen rectangular bands in the case with the slit and the Airy pattern for the circular aperture.

Central bright area - Airy disk - extends by reducing the aperture diameter, d. Through analyzing formula (7) or (12), we deduce that d-reduction results in increasing the angle, θ (while K and λ stay constant). Therefore, the smaller an aperture (and accordingly, telescope's mirror diameter), the bigger the Airy disk and the blurrier the Airy pattern (worse angular resolution of telescope). Hence, the constraint for astronomical observations is the size of a telescope. In order to resolve neighboring objects being closer to each other or the more distant ones, we need to build bigger telescopes.

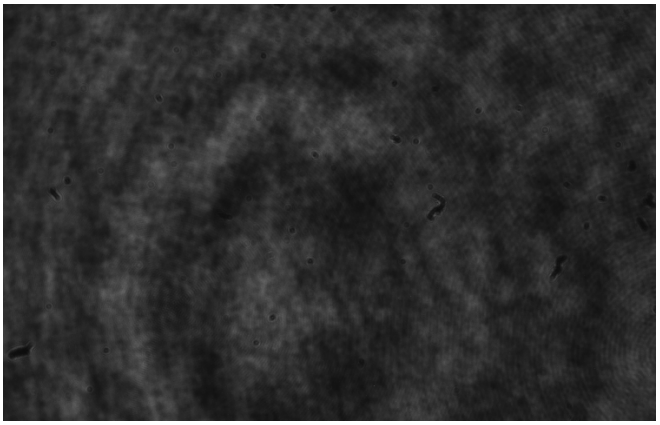

FIG. 3.— The dust in the optical system with visible diffraction pattern of its own.

When we take a closer look at the dust particles in the optical system (seen on the image shown in Figure 3), we can evidently notice that their own diffraction patterns are created. Diffraction is inevitable and occurs irregardless of size of a macroscopic obstacle that light rays encounter (for instance dust particles in this case or "anti"-slit in the experiments before). Dust introduces the next cause of inaccuracies in optical systems.

Proceeding with changing the set-up as described in the Method section, we place a coin on the light path. Figure 4 shows the pattern that can be observed on the wall. It consists of a shadow of the coin, with cricular fringes extending outward from its edge, and a bright spot in the center. The observation can be explained by taking into account a wave-nature of light, which predicts constructive interference at this point. According

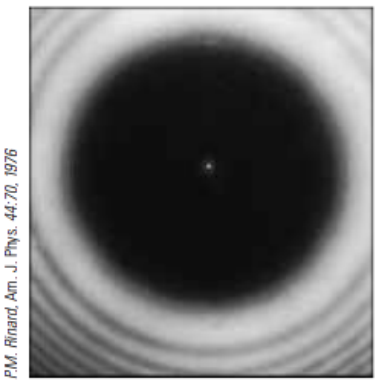

FIG. 4.— The Arago spot in the center of a diffraction pattern created by positioning a coin between the light source and the wall, from Serway & Jewett (2004).

TABLE 1
THE MINIMAL PHYSICAL OBJECT SIZE RESOLVED BY JWST FROM VARIOUS DISTANCES

Object	Distance	Distance (m)	Min. resolved size of the object (m)	Uncertainty (m)
Objects on the Earth ground	540 km	$5.40 \cdot 10^5$	$7.24 \cdot 10^{-2}$	$\pm 1.44 \cdot 10^{-2}$
Small solar structures	1 AU	$1.50 \cdot 10^{11}$	$2.01 \cdot 10^4$	$\pm 0.40 \cdot 10^4$
The Galactic Center	8.5 kpc	$2.62 \cdot 10^{20}$	$3.52 \cdot 10^{13}$	$\pm 0.70 \cdot 10^{13}$
A galaxy far away	$4 \cdot 10^9$ ly	$3.78 \cdot 10^{25}$	$5.07 \cdot 10^{18}$	$\pm 1.01 \cdot 10^{18}$

NOTE. — Magnitudes converted to SI base unit (meter) for comparison.

to Huygens' principle, each portion of the circumference of an obstacle - a coin - becomes a new point source of light waves. As the distance from each of these points to the center of the projected pattern is equal, we observe a constructive interference right in the center of a shadow - in the Arago spot (Serway & Jewett 2004).

The measured constant, K, and derived formula (12) are applied to the telescope with known parameters - James Webb Space Telescope. Its angular resolution is estimated to be in the range between $0.028''$ and $0.022'$, depending on the wavelength at which it will observe. Sources of light closer than this angular distance cannot be properly separetad, due to Rayleigh's criterion (the closest distance for which two different points can be resolved is when maximum of the diffraction pattern of on image coincides with the first minimum of another one), Serway & Jewett (2004). How small are objects that can be resolved by JWST from different distances, while observing with its best angular resolution? (See Table 1.)

First, we place the telesope in a near-Earth orbit (540km) to look at the objects on the ground. The magnitude of size of smallest resolved objects is then a couple of centimeters. This is an extremely high precision of observation, enabling location of very small items on the Earth's surface. In the second case, when JWST located at Earth is looking at the Sun, the spatial resolution is significantly worse, due to a larger distance. We increase the order of magnitude by placing JWST in the Solar System while observing the Galactic Center or looking at a galaxy formation far, far away. Obviously, observations conducted with JWST become more limited with the increasing distance, whreas objects that we are able to distinguish are larger. Thus, we do not expect to see an extraterrestial intelligent being reading a book somewhere in a galaxy 2 billion light years away, even if it was there.

REFERENCES

A summary of Error Propagation. (2007). Retrieved from: http : //ipl.physics.harvard.edu/wp − uploads/2013/03/ PS3_Error_Propagation_sp13.pdf

NASA, James Webb Space Telescope. (Accessed 2018). Retrieved from: https://jwst.nasa.gov/about.html

PHYWE series of publications. Laboratory Experiments. Diffraction intensity through a slit and a wire - Babinet's theorem. (2006). Retrieved from: *https : //www.nikhef.nl/ h73/kn1c/praktikum/ phywe/LEP/Experim/2_3_06.pdf*

Serway, R. A. and Jewett, J. W. (2004). Diffraction Patterns and Polarization. In *Physics for Scientists and Engineers* (pp.1205-1220). Thomson Brooks/Cole

Thorne, K. S. and Blandford, R. D. (2012). Diffraction. In *Applications of Classical Physics*. Retrieved from: http://www.pmaweb.caltech.edu/Courses/ph136/yr2012/